https://doi.org/10.48048/tis.2023.6431

# CFD Modeling for the Influence of Fly Ash Particle Size on the Different Properties of High Concentrated Slurry Transportation in Horizontal Pipe

**Yatish Kumar Baghel[*] and Vivek Kumar Patel**

*Motilal Nehru National Institute of Technology Allahabad, Prayagraj, India*

**([*]Corresponding author's e-mail: yatishbaghel@gmail.com)**

*Received: 4 October 2021, Revised: 5 December 2021, Accepted: 15 December 2021, Published: 30 November 2022*

**Abstract**

The disposal of fly ash from thermal power plants is becoming a serious concern for environmental engineers. This article attempts to study the influence of particle size of the fly ash on the various properties of high concentrated slurry (50 - 70 % by weight) flow through a horizontal pipe with the help of a commercial CFD code ANSYS FLUENT. Modified Herschel-Bulkley model and SST k-ω turbulence model is used for computational analysis, and the computational outcomes are validated with the available literature. In the present study, the fly ash samples were procured from different coal-based thermal power plants. Various properties: physical and rheological are obtained experimentally. The specific gravity of particles and the static settling concentration (SSC) of the slurry increases with the decrease in the particle size. The rheological properties increase as the concentration increases, and the slurry behaves like a non-Newtonian fluid at a high concentration. In addition, the particle size and concentration intensively impact on the skin friction coefficient and velocity distribution. However, no significant impact on the velocity profile at 70 % concentration (by weight).

**Keywords:** Yield stress, Bingham viscosity, Particle size, Rheological modeling, SST k-ω turbulence model, High concentration fly ash slurry flow

**Nomenclature**

| | |
|---|---|
| $C_w$ | concentration (by weight) |
| $D$ | pipe diameter |
| $f$ | mean skin friction coefficient |
| $K$ | consistency index |
| $k_s$ | roughness height |
| $L$ | pipe length |
| $n$ | power law index |
| $p$ | static pressure |
| $R_{eBc}$ | critical Bingham Reynolds number |
| $V$ | average flow velocity |
| $\mu_a$ | apparent viscosity |
| $\mu_o$ | yield viscosity |
| $\mu_B$ | Bingham viscosity |
| $\rho_m$ | density of slurry |
| $\bar{\bar{\tau}}$ | stress tensor |
| $\overline{\tau_o}$ | yield stress |

## Introduction

When it comes to the operation of thermal power plants, one of the most ecologically sensitive problems is coal ash management. For a nation like India, the ash percentage of local coal is relatively high, and as a result, an enormous amount of fly ash is produced in all thermal power plants [1]. There has been a significant growth in the effective consumption of fly ash for numerous purposes during the last couple of years. Therefore, major part of the fly ash is transported and stored through the energy efficient and environment friendly method. A pipeline transportation method for long distances is extensively used to transport solid materials: fly ash, coal, etc., in the form of slurry. In order to reduce

the consumption of energy and water in thermal power plant, it is wise to transport the slurry at a higher concentration [2]. The various types of slurry transportation systems can be classified based on their solid concentration (by weight), i.e., ($C_w \leq 20$ %) low concentration, ($C_w = 30$ - 40 %) medium concentration, and ($C_w \geq 50$ %) high concentration [3]. Chandel *et al.* [4]; Verma *et al.* [5,6]; Rawat *et al.* [7]; Singh *et al.* [8] conducted the experiment to evaluate the rheological properties of the fly ash slurry at high concentration with the help of a rheometer. They observed that the fly ash slurry acts as a non-Newtonian fluid at high concentrations and the rheological properties of the fly ash are affected by various factors such as the size of the solid particle, solid concentration, etc. Malin [9] developed the 2 turbulence models for Bingham plastic fluid flow in circular tubes. Bartosik [10] investigated the effect of the Herschel-Bulkley rheological model on the numerical prediction of turbulent flow of fine dispersive slurry. Furthermore, Bartosik [11] conducted the computational analysis for fine particle slurries at 0 to 45 % concentration (by volume). Haldenwang *et al.* [12] have investigated the Bingham plastic fluids flow in pipelines using both experimental as well as computational methods. Ling *et al.* [13] provided the numerical investigation of the slurry flow (double-species) in a horizontal pipe at various solid concentrations (by volume) range of 7.4 to 13.3 %. Ekambara *et al.* [14] used the kinetic theory of granular flows to predict the behavior of solid-liquid (slurry) in a horizontal pipeline using ANSYS-CFX. Further, an Eulerian approach for the modeling of multiphase flow and the RNG k- ε turbulent model used to analyze the slurry (coal-water) flow in a horizontal pipe is employed by Chen *et al.* [15]. Lin and Ebadian [16] studied flow properties distribution of the slurry flow at low concentration with the help of an Algebraic Slip Mixture in CFD in a horizontal pipe. Kaushal *et al.* [17] used the Mixture and the Eulerian multiphase models to find the pressure drop and velocity distribution in a pipe at different concentrations (up to 50 % by weight). CFD analysis of the slurry (mixture of water - sand) flow in a horizontal pipe at an overall volumetric concentration range of 15 - 45 % was performed by Gopaliya and Kaushal [18]. They analyzed the impact of particle size (sand) on various flow properties of the slurry flow using an Eulerian model and RNG k-ε turbulence model. Rawat *et al.* [19] determined the head loss of the flow (laminar and turbulent) of coal ash slurry in a horizontal pipe at a high concentration. Singh *et al.* [20] studied the flow properties of the slurry flow in a pipe through the CFD code FLUENT. Euler-Lagrange multiphase model and SST k-ω turbulence model were utilized to evaluate the flow properties. Singh *et al.* [21] studied the effect of the particle size and concentration (10 and 40 % by volume) of the slurry (sand - water) on the pressure drop in a horizontal pipe. Kumar *et al.* [22] computationally analyzed the velocity and concentration profiles of the fly ash slurry at low concentration in pipe with the help of Eulerian 2-phase model. During the slurry flow, various flow properties are influenced by slurry flow velocity [23]. Literature study shows that the most of the studies done on the modelling of the slurry flows are mainly focused on the low slurry concentration and Eulerian multiphase model, whereas the literature on the rheological modelling of the slurry flow at high concentration in horizontal pipe is scarce.

In the present investigation, the influence of particle size of the fly ash on the various properties is observed with the help of a commercial CFD code ANSYS FLUENT. The modified Herschel-Bulkley model and the SST k-ω turbulence model are used for computational analysis to evaluate flow properties. Initially, all the properties of the fly ash and slurry have been obtained experimentally. Further, CFD methodology is used to analyze the influence of different particle sizes and concentrations on the mean skin friction coefficient and visualize the velocity distribution for the laminar as well as the turbulent flow of slurry in a horizontal pipe at a higher concentration ($C_w \geq 50$ %).

**Procurement of the fly ash and instrumentations**

In the present investigation, fly ash is used as the solid particles in the slurry. The fly ash samples were procured from three different coal-based Indian thermal power plants, as given in **Table 1**. Thermal power plants produce different fly ash in term of particle size distribution (PSD). Hence, the PSD of the samples is found to differentiate the fly ash samples. The physical as well as rheological properties of the slurry are used in the CFD modeling to evaluate the flow properties of the slurry in the horizontal pipe.

**Table 1** Detail of the fly ash samples.

| Fly ash samples | Name of thermal power plant |
|---|---|
| Sample-1 (S-1) | National Thermal Power Corporation Unchahar, Uttar Pradesh, India |
| Sample-2 (S-2) | Prayagraj Power Generation Company Limited (Bara Thermal Power Plant) Prayagraj, Uttar Pradesh, India |
| Sample-3 (S-3) | Suratgarh Super Thermal Power Plant, Ganganagar, Rajasthan, India |

Therefore, initially all the properties of the slurry have been obtained through the experiments. Each experiment has been repeated four times in order to obtain average values of these properties with the consideration of various sources of errors. Various instruments were used in this investigation and **Table 2** shows the accuracy of the instruments. The accuracy of the weight measurement is ± 0.00001 gm.

**Table 2** Accuracy of the instruments.

| Instruments | Accuracy |
|---|---|
| pH meter | ± 0.01 |
| Rheometer | ± 0.0001 |
| Graduated cylinder | ± 0.1 |

PSD of the fly ash samples has been determined by utilizing the sieve and hydrometer analyses. The sieve analysis is used for coarse particles (> 75 μm), whereas for the fine particles (< 75 μm), the hydrometer analysis has been performed. A set of standard sieves (size, 300 - 75 μm) in the order of descending sizes was mounted on a mechanical shaker to sieve the samples. The weight of the retained sample on each sieve is measured, and a standard method is used to calculate the retained percentage on each sieve. After the sieve analysis, the hydrometer analysis is utilized to determine the PSD of the fly ash sample (< 75 μm) collected in the pan. After PSD, the specific gravity of solid particles is another significant property, and it is widely used for designing slurry transportation pipelines. In the present work, the specific gravity of the solid particles (fly ash) was evaluated by Pyknometer. The pH values for different fly ash slurries were prepared from different fly ash samples with different concentrations (50 - 70 % by weight) by using a pH meter (made by: Eutech Instruments Pte Ltd. Singapore). The pH values have been calculated after calibrating the meter with distilled water having a pH of 7.0. SSC is a parameter of great importance in order to determine the maximum solid concentration that can be allowed (with ± 5 % variation) to flow with the slurry in order to avoid chocking in the transportation lines. The SSC is the concentration of solids in the settled slurry, which depends on the specific gravity, shape and size of the particles of fly ash and the properties of the carrier fluid, like density and viscosity. In this investigation, the SSC was obtained through the gravitational settling phenomenon in a measuring cylindrical jar by taking a 30 % wt. concentration of the fly ash. The measurements have been taken by allowing the slurry to settle in the jar till a constant level of settled particles is achieved.

In estimating the energy needed to transport solid particles through pipelines, slurry viscosity is a significant parameter. The rheological properties of the slurry are determined at a higher concentration range (50 - 70 % by weight). The Rheogoniometer (Rheolab QC) from Anton Paar is used for rheological studies in a temperature-regulated workspace. In the current work, the PSD is evaluated by $d_{wm}$, and the values of $\tau_o$ and $\mu_B$ obtained from the experiment for the various $d_{wm}$ are utilized as input parameters for the computational analysis.

## Mathematical modelling

### Governing equations and turbulence modeling

The governing equations representing the problem physics are solved during the CFD analyses and are given in Eqs. (1) - (4). Eq. (1) represents the continuity equation.

$$\nabla.(\rho\vec{u}) = 0 \quad (1)$$

The expression for momentum conservation is given in Eq. (2).

$$\nabla.(\rho\vec{u}\vec{u}) = -\nabla p + \nabla.(\overline{\overline{\tau}}) \tag{2}$$

Eq. (3) shows the expression of $\overline{\overline{\tau}}$ for laminar flow of a Bingham fluid.

$$\overline{\overline{\tau}} = \overline{\tau_o} + \mu_B \overline{\overline{D}} \tag{3}$$

where, $\overline{\overline{D}} = (\frac{\partial U_j}{\partial x_i} + \frac{\partial U_i}{\partial x_j})$ (4)

A comparative study of different turbulent models has been carried out in order to obtain a best suited model for the problem. The Eqs. (5) - (15) of the Shear Stress Transport model (SST k-ω) are imitated from Dewan [24].

$$\overline{u_j}\frac{\partial k}{\partial x_j} = \frac{\partial}{\partial x_j}[(\nu + \sigma_k \nu_t)\frac{\partial k}{\partial x_j}] + P_k - \beta^* k\omega \tag{5}$$

$$\overline{u_j}\frac{\partial \omega}{\partial x_j} = \frac{\gamma P_k}{\rho \nu_t} - \beta\omega^2 + \frac{\partial}{\partial x_j}[(\nu + \sigma_\omega \nu_t)\frac{\partial \omega}{\partial x_j}] + 2(1-F_1)\sigma_{\omega 2}\frac{1}{\omega}\frac{\partial k}{\partial x_j}\frac{\partial \omega}{\partial x_j} \tag{6}$$

where, the turbulent viscosity is given by Eq. (7).

$$\nu_t = \frac{a_1 k}{\max(a_1\omega, SF_2)} \tag{7}$$

$$P_k = \min[\frac{\partial \overline{u_i}}{\partial x_j}, 10\beta^* k\omega] \tag{8}$$

Eqs. (8) - (11) represent the different relations and model constant.

$$F_1 = \tanh(\{\min[\max(\frac{\sqrt{k}}{\beta^* y\omega}, \frac{500\nu}{y^2\omega}), \frac{4\sigma_{\omega 2}k}{y^2 CD_{k\omega}}]\}^4) \tag{9}$$

$$CD_{k\omega} = \max(2\rho\sigma_{\omega 2}\frac{1}{\omega}\frac{\partial k}{\partial x_j}\frac{\partial \omega}{\partial x_j}, 10^{-20}) \tag{10}$$

$$F_2 = \tanh(\max(\frac{2\sqrt{k}}{\beta^* y\omega}, \frac{500\nu}{y^2\omega})^2) \tag{11}$$

Constant terms in the SST k-ω model are generated by combining the k-ε and k-ω models constant, such as a constant ( $\phi$ ) may be acquired by the following relationship:

$$\phi = \phi F_1 + \phi_2(1 - F_1) \tag{12}$$

$$\gamma_1 = \frac{\beta_1}{\beta^*} - \frac{\sigma_{\omega 1}k^2}{\sqrt{\beta^*}}, \gamma_1 = \frac{\beta_2}{\beta^*} - \frac{\sigma_{\omega 2}k^2}{\sqrt{\beta^*}} \tag{13}$$

$$\beta_1 = 0.075, \beta_2 = 0.0828, \beta^* = 0.09 \tag{14}$$

$$\sigma_{k1} = 0.85, \sigma_{k2} = 1, \sigma_{\omega 1} = 0.5, \sigma_{\omega 2} = 0.856, a_1 = 0.31 \tag{15}$$

The detail and specification of various term of this model are found in Dewan [24]; Fluent [25]; Menter [26].

**Geometry and grid generation**

The computational domain has been modeled by using 2 dimensions: L = 7 m and D = 50 mm. Based on the works by Brown and Heywood [27]; Wasp *et al.* [28], the computational domain entry length, $x/D \geq 50$, is used to obtain the fully developed turbulent flow. ANSYS ICEM CFD software is used to generate the grid of the computational flow domain. The computation domain was discretized using a multi-block unstructured, non-uniform grid system with hexahedral elements, as illustrated in **Figure 1**, and fine grids are required along the wall for effective assessment.

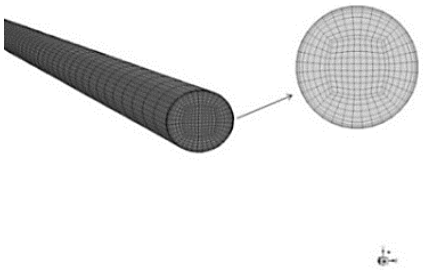

**Figure 1** Computational flow domain.

**Table 3** Grid independency test.

| Number of element | Pressure drop (mWc/100 m) | % variation |
|---|---|---|
| 9,295 | 64.1125 | |
| 18,590 | 63.9462 | 0.26 |
| 37,100 | 63.7025 | 0.38 |
| 56,880 | 62.8361 | 1.36 |
| 84,800 | 62.7975 | 0.061 |
| 149,320 | 62.7951 | 0.00328 |

A grid independence test (GIT) is conducted by varying the number of elements from 9,000 to 150,000 in order to determine the optimum grid size as shown in **Table 3**. The GIT shows that the pressure gradient values do not change significantly beyond 84,800 elements in the fully developed region. Hence, the grid size of 84,800 elements was selected for further investigations.

**Boundary control and solution control**

There are 3 boundary conditions applied to the computational flow domain: Inlet, outlet and wall. A uniform velocity and outflow are provided at the pipe's inlet and outlet, respectively, as the boundary conditions. A no-slip boundary condition with a wall roughness constant of 0.5 is applied to the pipe wall. The first-order upwind scheme is used to discretize the governing equations as it leads to better stability, accuracy and convergence than other schemes. For coupling the pressure-velocity equations, a SIMPLE algorithm is used. To prevent solution divergence, the under-relaxation method has been adopted for all the dependent variables. $10^{-6}$ is taken as convergence criteria for solution parameters (velocity components, turbulent kinetic energy and specific dissipation rate).

**Rheological modeling**

Many studies on the rheology of the fly ash (Elliot [29]; Wilson [30]) suggest that the slurry flowing through the pipes behaves like a homogeneous suspension at higher concentrations. Bunn *et al.* [31] observed that the fly ash slurries are similar to non-Newtonian behavior at higher concentrations. Following changes to the Herschel-Bulkley model, the Herschel-Bulkley model is rendered comparable to the Bingham plastic model in the ANSYS FLUENT software. The equation of the Bingham plastic fluids can be given as;

$$\tau = \tau_o + \mu_B \dot{\gamma} \tag{16}$$

The equation of Herschel-Bulkley model in ANSYS FLUENT is given by

$$\tau = \mu_a \dot{\gamma} = \tau_o + K[\dot{\gamma}^n - (\frac{\tau_o}{\mu_o})^n] \tag{17}$$

The Herschel-Bulkley model behaves like a Bingham plastic model if $n = 1$, $K = \mu$, and $(\tau_0/\mu_0) \rightarrow 0$. Gertzos *et al.* [32] analyzed that the above-mentioned conditions could be achieved at a higher value of $\mu_0$. In the present study, $\mu_0$ is assigned as $10^{10}$ for the numerical analysis. There are 2 non-dimensional numbers, such as the Hedstrom number ( $H_e$ ) and the Bingham Reynolds number ( $R_{eB}$ ) are utilized in the present work. Eqs. (18) - (19) represent the $H_e$ and $R_{eB}$ numbers, respectively. In the present analysis, the different values of $H_e$ and $R_{eB}$ are determined by changing the magnitudes of $\tau_0$ and $\mu_B$ .

$$H_e = \frac{D^2 \tau_o \rho_m}{\mu_B^2} \tag{18}$$

$$R_{eB} = \frac{\rho_m V D}{\mu_B} \tag{19}$$

**Validation of the CFD results**

The computational methodology is validated with the experimentally obtained results given by Chandel *et al.* [4]. When comparing the computational outcomes with the experimental results, the pipeline roughness in each test loop has to be determined first in order to compare the findings. Chandel *et al.* [4] have compiled a large amount of information on the pressure drop associated with the water flow and calculated the roughness of the pipe loop ($k_s$/D). It was revealed that the pipe utilized by Chandel *et al.* [4] had a $k_s$/D of $10^{-4}$. Therefore, the same has been taken for further computational analysis. Hanks [33] proposed a condition to evaluate whether a slurry flow is laminar or turbulent. According to the condition, the flow is considered laminar for $R_{eB} < R_{eBC}$ and turbulent otherwise. Eq. (9) represents the critical Bingham Reynolds number ( $R_{eBC}$ ). As per the condition, for the data given by Chandel *et al.* [4] at 60 % concentration (by weight), the flow is found turbulent at all the used velocities. Therefore, fly ash slurry is assumed to be a single homogeneous phase for the current numerical simulations at high concentrations.

$$\mathrm{R}_{eBC} = \left(\frac{H_e}{8x_c}\right)\left[1 - \frac{4x_c}{3} + \frac{x_c^4}{3}\right] \tag{20}$$

$$\text{where, } \frac{x_c}{(1-x_c)^4} = \frac{H_e}{16800} \tag{21}$$

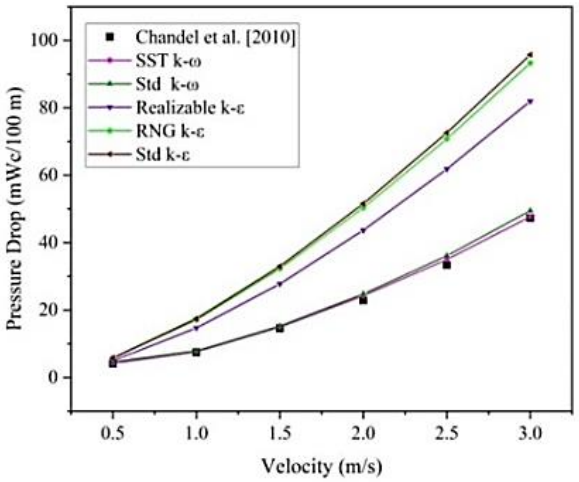


**Figure 2** Validation of the computational models with the experimental data.

**Figure 2** represents the validation of the computational models with the experimental data [4]. At 60 % wt. concentration, the pressure drop/100 m length of a pipe is calculated along the fully developed region at different velocities of slurry flow.

**Error analysis**

The maximum percentage error for Standard k-ε, Realizable k-ε and RNG k-ε are show as 133.98, 129.01 and 96.57 %, respectively. However, the maximum percentage error for SST k-ω and Standard k-ω turbulence models is 6.13 and 14.35 %, respectively. Standard method is used to calculate the % error between computational results and experimental results. It is seen that the computational results yielded by applying the SST k-ω model resembled the experimental results to the closest. Therefore, the SST k-ω model is employed for further analysis. In addition, the assumption that the high concentration slurry is similar to a single homogenous phase fluid is also evidently verified from the validation. Hence, the same can be used for further analysis confidently.

## Results and discussion

**Evaluation of the properties of the fly ash slurry**

Properties of the fly ash samples have been evaluated based on the methods discussed in previous section. **Table 4** represents the PSD of all 3 samples through the experimental methods. It is observed that the top particle size of the samples S-1 and S-2 is 300 µm, and 54.95 and 60.5 % of the particles are found to be finer than 75 µm for the samples S-1 and S-2, respectively. Whereas for the sample S-3, 212 µm is the size of particles at the top, and 70.25 % of particles are found at a size of less than 75 µm. After the analyses, the weighted mean diameters ($d_{wm}$) of the particles have been calculated as given in **Table 5.** The specific gravity (obtained by an experimental evaluation) of all the fly ash samples is presented in **Table 5**.

**Table 4** PSD of the fly ash samples.

| | | | | | | | | | | |
|---|---|---|---|---|---|---|---|---|---|---|
| Size (micron) | 300 | 250 | 212 | 150 | 106 | 75 | 36 | 16.58 | 11.25 | 4.64 |
| S-1 | 99.35 | 97.75 | 95.65 | 86.25 | 69.75 | 54.95 | 29.75 | 7.5 | 5.5 | 2.74 |
| Size (micron) | 300 | 250 | 212 | 150 | 106 | 75 | 36 | 14.09 | 9.53 | 6.63 |
| S-2 | 99.9 | 98.75 | 97.25 | 88.5 | 74.75 | 60.5 | 31.25 | 9.15 | 7.46 | 4.5 |
| Size (micron) | 300 | 250 | 212 | 150 | 106 | 75 | 36 | 22.76 | 13.56 | 7.79 |
| S-3 | 100 | 100 | 99.75 | 92.75 | 83.5 | 70.25 | 38.12 | 18.25 | 6.25 | 4.25 |

The measured specific gravity values range between 2.062 to 2.475 for each power plant fly ash sample; the highest value is found for the sample S-3 (with the least weighted mean diameter of 50.8 µm).

**Table 6** shows the determined pH values for all 3 fly ash samples. The range of the pH values is found to be 7.01 - 7.03, which is indicative of all the samples being non-reactive. In addition, it is further observed that the pH values do not significantly vary with the concentration.

**Table 5** Specific gravity and weighted mean diameter of the fly ash samples.

| Fly ash samples | S-1 | S-2 | S-3 |
|---|---|---|---|
| Specific gravity | 2.062 | 2.114 | 2.475 |
| Weight mean diameter ($d_{wm}$) in micron | 68.07 | 60.68 | 50.8 |

**Table 6** pH value of the different slurry samples.

| Fly ash samples | S-1 | S-2 | S-3 |
|---|---|---|---|
| At $C_w$ = 50 % | 7.01 | 7.01 | 7.02 |
| At $C_w$ = 60 % | 7.02 | 7.01 | 7.02 |
| At $C_w$ = 70 % | 7.02 | 7.02 | 7.03 |

The values of SSC for the different samples (S-1, S-2 and S-3) are obtained as 65.5, 66.67 and 68.75 % (by weight), respectively. **Figure 3** represents the variation of the SSC with respect to time. It is seen that the settling rate of the sample S-3 is the lowest because it has the largest number of finer particles (< 75 μm).

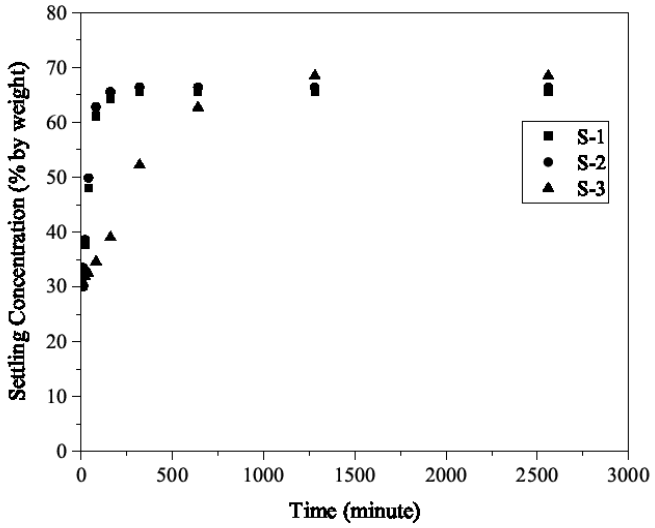


**Figure 3** Variation of SSC of the slurry samples.

It is found in previous studies that the slurry is similar to non-Newtonian fluid at a concentration ($C_w$) of 40 % and above (Verkerk [34]; Sive and Lazarus [35]; Biswas *et al.* [36]). **Table 7** represents the rheological results of the slurry samples, and the slurry samples represent the Bingham Plastic fluid from various types of non-Newtonian fluid. It is observed that the rheological properties increase with the increase in concentration and the slurry samples represent the Bingham plastic behavior of the non-Newtonian fluid. The PSD of the fly ash particles and the concentration (by weight) have a significant effect on the $\tau_o$ and $\mu_B$ values [6].

**Table 7** Rheological properties of the different slurry samples at 28 ℃ temperature.

| $C_w$ (by weight) | Yield stress (Pa) ( $\tau_o$ ) | Slurry viscosity (Pa s) ( $\mu_B$ ) | Water viscosity (Pa s) | Remark |
|---|---|---|---|---|
| **S-1** | | | | |
| 50 % | 1.8092 | 0.017 | 0.891 | Non-Newtonian |
| 60 % | 4.523 | 0.0426 | 0.891 | Non-Newtonian |
| 70 % | 8.0798 | 0.3161 | 0.891 | Non-Newtonian |
| **S-2** | | | | |
| 50 % | 1.0269 | 0.0244 | 0.891 | Non-Newtonian |
| 60 % | 3.4229 | 0.0747 | 0.891 | Non-Newtonian |
| 70 % | 12.865 | 0.5136 | 0.891 | Non-Newtonian |
| **S-3** | | | | |
| 50 % | 1.1219 | 0.044 | 0.891 | Non-Newtonian |
| 60 % | 3.7395 | 0.1466 | 0.891 | Non-Newtonian |
| 70 % | 33.875 | 0.6764 | 0.891 | Non-Newtonian |

**Effect of particle size and concentration on the skin friction coefficient**

The skin friction coefficient in the slurry flow through a horizontal pipe at a high concentration (50 - - 70 % by weight) and different velocities (1 - 3 m/s) has been calculated. By applying the Hanks [33] condition, it is found that at $C_w$ = 50 %, the flow is laminar at 1 m/s only for the samples S-1 and S-3, and the flow is found to be turbulent for all the samples at velocities greater than 1 m/s. At $C_w$ = 60 %, the flow of sample S-1 is found to be laminar up to 1.5 m/s velocities and turbulent beyond 1.5 m/s, whereas for sample S-2, the flow is laminar for the velocity range of 1-2 m/s and turbulent beyond 2 m/s.

Similarly, for sample S-3, the flow is laminar at all velocities. At $C_w$ = 70 %, the flow is found to be laminar at all velocities for all the samples. **Figure 4** represents the variation of the mean skin friction coefficient (*f*) of the slurry samples at different concentrations. It is observed that the *f* decreases with the increase in velocity at a given concentration for both the flows: Laminar as well as turbulent. It is also observed that the *f* increases with the concentration at a given velocity. **Figure 5** represents the influence of the particle size on the *f* at different concentrations. At 50 % wt. concentration, the value of *f* at 1 m/s is less as compared to 1.5 m/s velocity in samples S-1 and S-3 due to the flow changing from laminar to turbulent, but in S-2, there is turbulent flow at all velocities, hence *f* is decreasing with the increase in velocity.

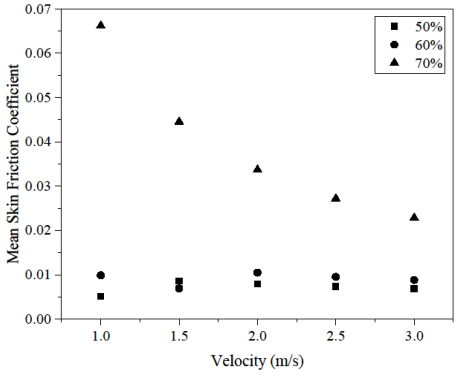


(a)

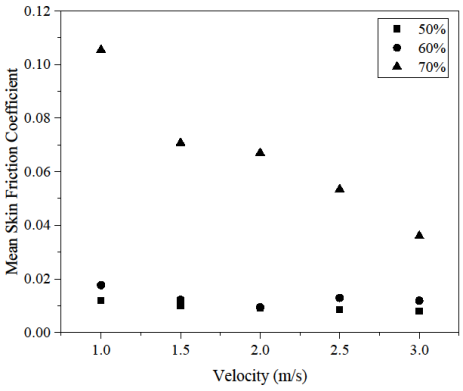


(b)

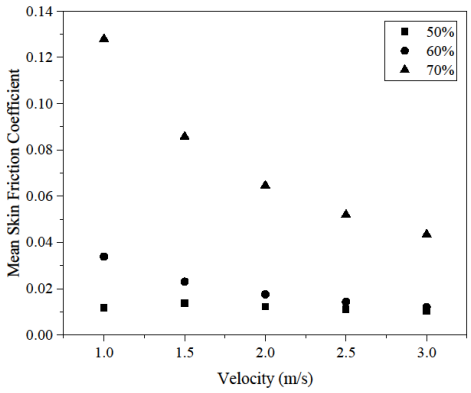


(c)

**Figure 4** Variation of mean skin friction coefficient of the slurry samples at different concentrations, (a) = S-1, (b) = S-2, (c) = S-3.

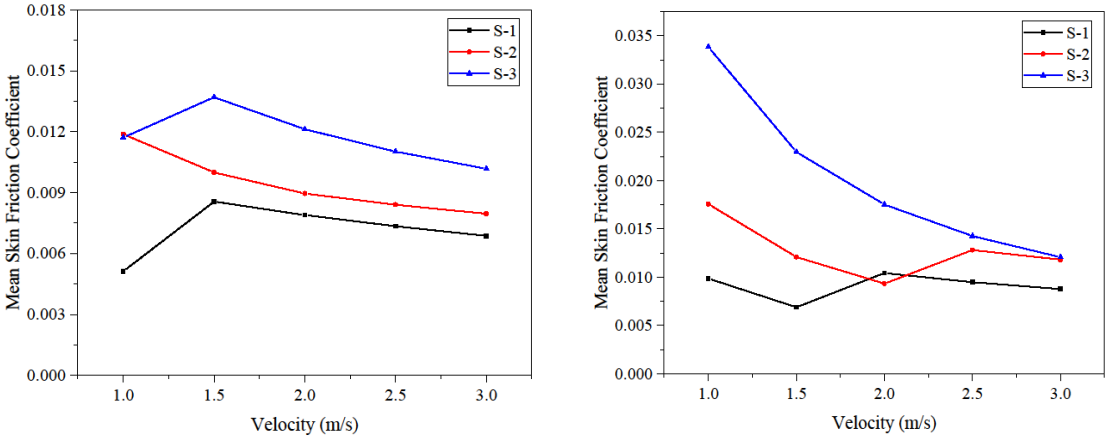


(a) (b)

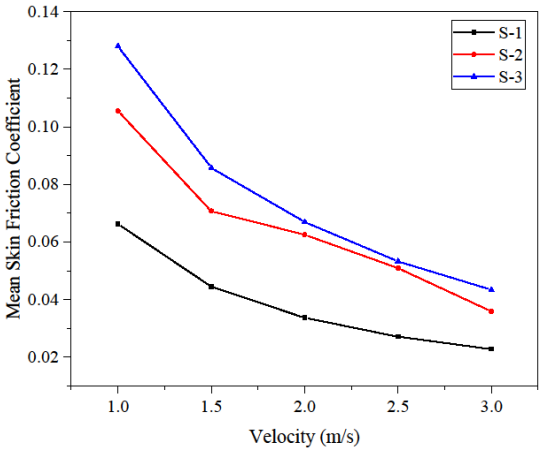


(c)

**Figure 5** Influence of particle size on the mean skin friction coefficient of the slurry samples at different concentrations (a) $C_w$ = 50 %, (b) $C_w$ = 60 %, (c) $C_w$ = 70 %.

Similarly, this happened in samples S-1 and S-2 at 2 m/s velocity. At 70% concentration, it is clearly observed that the *f* is decreasing with the increase in velocity in all samples at every velocity. It is also seen that the S-3 has more *f* as compared to the other samples at all concentrations. Hence, subsequently it can be concluded that the *f* is intensively dependent on the fly ash particle size in the flow of slurry.

**Effect of particle size and concentration on the velocity distribution**

Various parameters: viscosity, size and shape of the fly ash particles as well as velocity and concentration of the slurry, etc., impact the velocity distribution (profile) of the flow of slurry in the pipe. **Figures 6 - 8** represents the influence of particle size on the velocity distribution of the slurry at different concentrations.

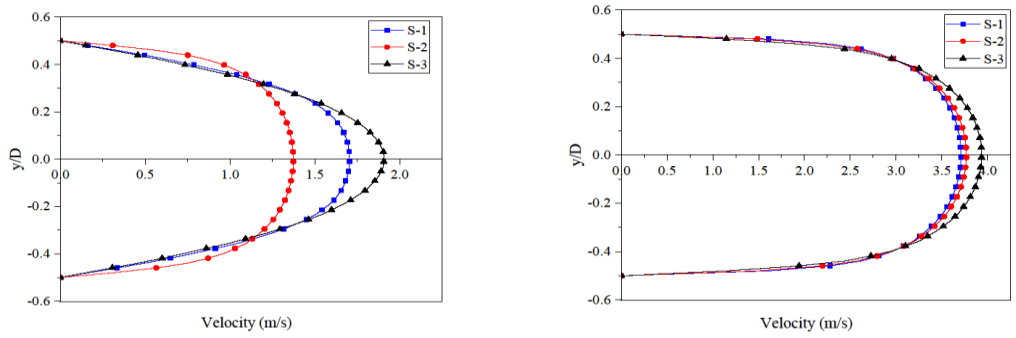


(a) (b)

**Figure 6** Influence of particle sizes on the velocity distributions of the slurry samples at $C_w$ = 50 %, (a) V = 1 m/s, (b) V = 3 m/s.

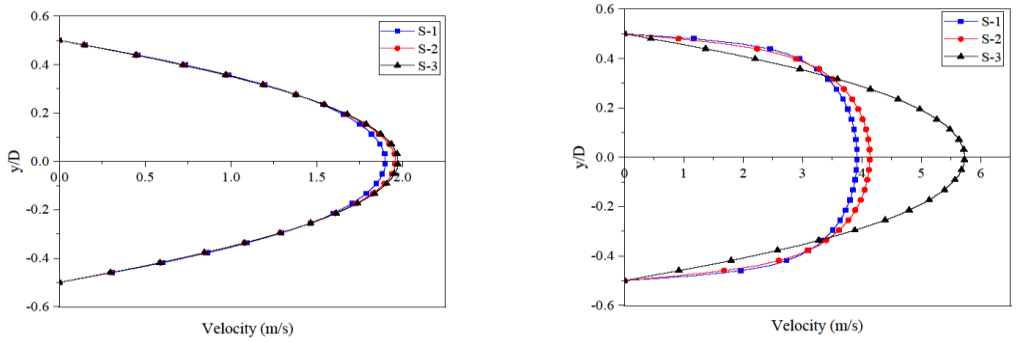


(a) (b)

**Figure 7** Influence of particle sizes on the velocity distributions of the slurry samples at $C_w$ = 60 %, (a) V = 1 m/s, (b) V = 3 m/s.

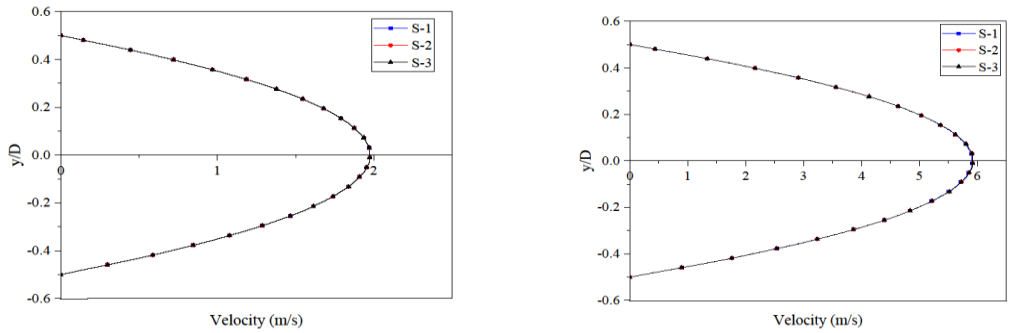


**Figure 8** Influence of particle sizes on the velocity distributions of the slurry samples at $C_w$ = 70 %, (a) V = 1 m/s, (b) V = 3 m/s.

For 50 % concentration, Samples S-1 and S-3 represent the velocity profile of laminar flow, and samples 2 shows the velocity profile of turbulent flow at 1 m/s velocity while at 3 m/s velocities, all the velocity profiles for turbulent flow in all samples. At 60 % concentration, all samples show the velocity profile for laminar flow at 1m/s velocity and at 3 m/s, the samples S-1 and S-2 represent turbulent flow, whereas S-3 shows the laminar flow. Similarly, at 70 % concentration, all samples represent the velocity profile for laminar flow at given velocities (1 and 3 m/s). The trend of the velocity profiles is followed by the velocity profile for Bingham plastic fluid in the horizontal pipe suggested by Govier and Aziz [37]. The flow of slurry behaves like a homogenous at a high concentration of solid, and this is the reason for the symmetry of the velocity profile. **Figures 6 - 7** show that the velocity profile is compressing towards the origin as the particle size is increased in different fly ash samples for the same concentration and flow velocity. The particle sizes and concentration do not show a significant effect on the velocity profile at a very high concentration (70 % by weight) as shown in **Figure 8**. Still, the impact on the friction factor is found to be significant.

## Conclusions

The following inferences can be concluded from the present study: Fly ash slurry samples from different thermal power plants represent the variation in the PSD and SSC. The samples also show the variation in specific gravity and size of the solid particles of the fly ash. There is no significant impact of particle size and concentration on the pH value of the slurry samples. The magnitude of $\tau_o$ and $\mu_B$ increases with the increase in concentration and is more pronounced at very high concentration (70 % by weight). At a high concentration ($C_w$ > 40 % by weight), the behavior of slurry samples like a non-Newtonian fluid has been confirmed, and the assumption that the high $C_w$ fly ash slurry is similar to a single homogenous phase fluid is also evidently verified. In the turbulent flow, the SST k-ω turbulence model was found most to be the most appropriate when compared to the other turbulence models. At a given concentration, *f* decreases as velocity increases. Sample S-3 of the lowest particle size has more mean skin friction coefficient as compared to the other samples at all concentrations. At high concentration, the slurry behaves like a homogenous mixture due to which the velocity profile is symmetrical. The velocity profile is compressing towards the origin as the particle size is increased in different fly ash samples for a concentration and flow velocity. The particle sizes and concentration do not show a significant effect on the velocity profile at very high concentration (70 % by weight), but the effect on friction factor is significant.

## Acknowledgements

The authors thankfully acknowledge to the Indian Institute of Technology Delhi, India for rheological testing.

**References**


[1] S Jayanti, K Maheswaran and V Saravanan. Assessment of the effect of high ash content in pulverized coal combustion. *Appl. Math. Model*. 2007; **31**, 934-53.

[2] SN Singh. Wet disposal of coal ash at higher concentrations. *In*: Proceedings of the 1st International Conference on Flyash Utilization, New Delhi, India. 2011.

[3] S Chandel, V Seshadri and SN Singh. Effect of additive on pressure drop and rheological characteristics of fly ash slurry at high concentration. *Particulate Sci. Tech*. 2009; **27**, 271-84.

[4] S Chandel, SN Singh and V Seshadri. Pilot Plant test loop facility for performance characteristics of centrifugal slurry pumps at high concentrations. *In*: Proceedings of the International Conference on Emerging Trends in Engineering and Technology, Kurukshetra, India. 2010, p. 14-6.

[5] AK Verma, SN Singh and V Seshadri. Pressure drop prediction for the flow of fly ash slurries through pipes at high concentrations. *Int. J. Fluid Mech. Res.* 2010; **37**, 295-304.

[6] AK Verma, SN Singh and V Seshadri. Effect of particle size distribution on rheological properties of fly ash slurries at high concentrations. *Int. J. Fluid Mech. Res.* 2006; **33**, 445-57.

[7] A Rawat, SN Singh and V Seshadri. Variation of physical and rheological properties of fly ash slurries with particle size and its effect on hydraulic transportation at high concentrations. *Particulate Sci. Tech*. 2019; **37**, 151-60.

[8] DB Singh, N Kumar, DR Kaushal, AK Sharma and JK Yadav. Effect of solid concentration and grain size on the rheology of fly ash slurries. *Mater. Today Proc.* 2021; **46**, 10904-8.

[9] MR Malin. The turbulent flow of Bingham plastic fluids in smooth circular tubes. *Int. Comm. Heat Mass Tran*. 1997; **24**, 793-804.

[10] A Bartosik. Modelling of a turbulent flow using the Herschel-Bulkley rheological model. *Inzynieria Chemiczna i Procesowa*. 2006; **27**, 623.

[11] AR Bartosik. Simulation of turbulent flow of a fine dispersive slurry. *Chem. Process. Eng*. 2010; **31**, 67-80.

[12] R Haldenwang, APN Sutherland, VG Fester, R Holm and RP Chhabra. Sludge pipe flow pressure drop prediction using composite power-law friction factor-Reynolds number correlations based on different non-Newtonian Reynolds numbers. *Water SA* 2012; **38**, 615-22.

[13] J Ling, CX Lin and MA Ebadian. Numerical investigations of double-species slurry flow in a straight pipe entrance. *In*: Proceedings of the ASME International Mechanical Engineering Congress and Exposition, Louisiana, USA. 2002, p. 145-54.

[14] K Ekambara, RS Sanders, K Nandakumar and JH Masliyah. Hydrodynamic simulation of horizontal slurry pipeline flow using ANSYS-CFX. *Ind. Eng. Chem. Res*. 2009; **48**, 8159-71.

[15] L Chen, Y Duan, W Pu and C Zhao. CFD simulation of coal-water slurry flowing in horizontal pipelines. *Korean J. Chem. Eng*. 2009; **26**, 1144-54.

[16] CX Lin and MA Ebadian. A numerical study of developing slurry flow in the entrance region of a horizontal pipe. *Comput. Fluid*. 2008; **37**, 965-74.

[17] DR Kaushal, T Thinglas, Y Tomita, S Kuchii and H Tsukamoto. CFD modeling for pipeline flow of fine particles at high concentration. *Int. J. Multiphas. Flow* 2012; **43**, 85-100.

[18] MK Gopaliya and DR Kaushal. Analysis of effect of grain size on various parameters of slurry flow through pipeline using CFD. *Particulate Sci. Tech*. 2015; **33**, 369-84.

[19] A Rawat, SN Singh and V Seshadri. Computational methodology for determination of head loss in both laminar and turbulent regimes for the flow of high concentration coal ash slurries through pipeline. *Particulate Sci. Tech.* 2016; **34**, 289-300.

[20] JP Singh, S Kumar and SK Mohapatra. Modelling of two phase solid-liquid flow in horizontal pipe using computational fluid dynamics technique. *Int. J. Hydrogen Energ*. 2017; **42**, 20133-7.

[21] V Singh, S Kumar and D Ratha. Slurry flow characteristics numerically analysed using sand water mixture. *AIP Conf. Proc.* 2021; **2341**, 030038.

[22] N Kumar, DR Kaushal, VK Dwivedi, DB Singh, SK Sharma and JK Yadav. CFD modeling of fly-ash slurry to analyse the concentration and velocity profiles. *Mater. Today Proc.* 2020; **21**, 1695-9.

[23] G Feng, Z Wang, T Qi, X Du, J Guo, H Wang and X Wen. Effect of velocity on flow properties and electrical resistivity of cemented coal gangue-fly ash backfill (CGFB) slurry in the pipeline. *Powder Tech*. 2021; **396**, 191-209.

[24] A Dewan. *Tackling turbulent flows in engineering.* Springer, Berlin, Germany, 2011.

[25] ANSYS fluent. *ANSYS fluent 12.0: User's guide.* ANSYS fluent, 2011.

[26] FR Menter. Two-equation eddy-viscosity turbulence models for engineering applications. *AIAA J.* 1994; **32**, 1598-605.
[27] NP Brown and NI Heywood. *Slurry handling: Design of solid-liquid systems.* 1st ed. Elsevier Science Publishing, New York, 1991.
[28] EJ Wasp, JP Kenny and RL Gandhi. *Solid-liquid flow slurry pipeline transportation.* Gulf Publishing, Houston, USA, 1979.
[29] DE Elliot. Hydraulic transport of coal ash at high concentration. *In*: Proceedings of the International Conference on the Hydraulic Transport of Solids in Pipes; BHRA (Association), Bedford, UK. 1970, p. 25-6.
[30] KC Wilson. Dense-phase option for coarse-coal pipelining. *J. Pipelines* 1982; **2**, 95-101.
[31] T Bunn, AJ Chambers and CM Goh. Rheology of some flyash slurries. *Powder Handling Process*. 1991; **3**, 221-6.
[32] KP Gertzos, PG Nikolakopoulos and CA Papadopoulos. CFD analysis of journal bearing hydrodynamic lubrication by Bingham lubricant. *Tribol. Int.* 2008; **41**, 1190-204.
[33] RW Hanks. On the flow of Bingham plastic slurries in pipes and between parallel plates. *Soc. Petrol. Eng. J*. 1967; **7**, 342-6.
[34] CG Verkerk. Transport of fly ash slurries. *BHRA Fluid Eng.* 1982; **8**, 307-16.
[35] AW Sive and JH Lazarus. *Hydraulic transport system design for high concentration fly ash slurries.* Pretoria, South Africa, 1987.
[36] A Biswas, BK Gandhi, SN Singh and V Seshadri. Characteristics of coal ash and their role in hydraulic design of ash disposal pipelines. *Indian J. Eng. Mater. Sci.* 2010; **7**, 1-7.
[37] GW Govier and K Aziz. *The flow of complex mixtures in pipes.* Van Nostrand Reinhold, New York, 1972.